

## Constraining the Nucleon EDM due to BSM on the Lattice

---

**Thomas Luu**<sup>a,b,\*</sup>

<sup>a</sup>*Institute for Advanced Simulation (IAS-4) & JARA, Forschungszentrum Jülich, Germany*

<sup>b</sup>*Helmholtz-Institut für Strahlen- und Kernphysik, Rheinische Friedrich-Wilhelms-Universität Bonn, Germany*

*E-mail:* [t.luu@fz-juelich.de](mailto:t.luu@fz-juelich.de)

We discuss how lattice QCD calculations are used to calculate the induced nucleon electric dipole moment due to various flavor-diagonal CP-violating operators, some of which originate from beyond the standard model. We describe the implications of symmetries, and lack thereof, of the lattice action and the operators used to measure the electric dipole moment.

*RDP online PhD school and workshop "Aspects of Symmetry"(Regio2021),  
8-12 November 2021  
Online*

---

\*Speaker

## 1. Introduction

The Standard Model of Particle Physics (SM) has been widely successful in describing the measured particle spectrum and composition of matter ranging from quarks and gluons to multi-hadron systems. Such systems constitute approximately 5% of the observable matter-energy within the Universe. Yet the theory alone cannot explain the origins of the remaining 95% of matter and energy, dubbed ‘Dark Matter’ and ‘Dark Energy’, respectively. Further, the Standard Model does not provide the requisite amount of charge-conjugation and parity (CP) violation to account for the observed matter/anti-matter asymmetry. Therefore any physical description of such phenomena requires a theory that goes *beyond* the Standard Model (BSM), while at the same time encompassing the Standard Model and its predictions related to ordinary matter.

BSM theories all share certain operator traits that can be utilized in a formal study involving lattice stochastic methods of QCD. When viewed as a low-energy effective theory of some larger (still unknown) fundamental theory, the Standard Model, consisting of renormalizable operators of dimension 4 or less, is augmented with BSM operators of dimension  $> 4$ . The structures of these higher dimension operators can be determined generically assuming the larger fundamental theory respects certain symmetries (e.g. CPT and gauge invariance). Different candidate BSM theories will give different couplings for these higher-dimensional operators. When BSM theories are expressed in this manner, all the benefits inherent to effective field theories (EFTs) follow through, such as a hierarchy in operator complexity and a systematic power counting of terms. Throughout the world experiments are taking place that aim to measure higher-dimensional operators stemming from BSM theories via precision experiments.

But why do we need to involve QCD, let alone a discretized stochastic version of QCD, if we are interested in physics that is BSM? The answer comes from how we intend to observe the effects of BSM. BSM physics manifest themselves in small, minute changes in select properties of hadronic systems. Because hadrons themselves are governed by QCD (as well as other forces), a careful and precise accounting of the QCD aspect of these hadronic systems is needed if we are to disentangle BSM physics from their QCD component. And because QCD is strongly interacting in this hadronic low-energy regime, *lattice* QCD (LQCD) is required since it is the only method that is able to tackle this non-perturbative regime.

Some prime examples of where BSM physics can induce small changes in hadronic properties are in measurements of the muon anomalous magnetic moment ( $g-2$ ) and the nucleon electric dipole moment (nEDM). In the former case, though the muon is not a hadron, the contribution to its magnetic moment  $g$  involves hadronic components, such as through vacuum polarization (see, e.g., [1] and references within). Here BSM can potentially induce a value of  $g$  that differs from a pure standard model prediction. Current measurements of  $g-2$  do suggest the possibility of BSM physics [2, 3], and at this point the largest systematic uncertainty in calculations of this quantity is due to its hadronic component.

If a non-zero measurement of the nEDM were obtained with today’s experiments, this could also give a very strong argument for the presence of BSM. As the nucleon is the quintessential hadron, it is governed predominantly by QCD and thus LQCD is essential in simulating this system. The nEDM will be discussed in more detail shortly.

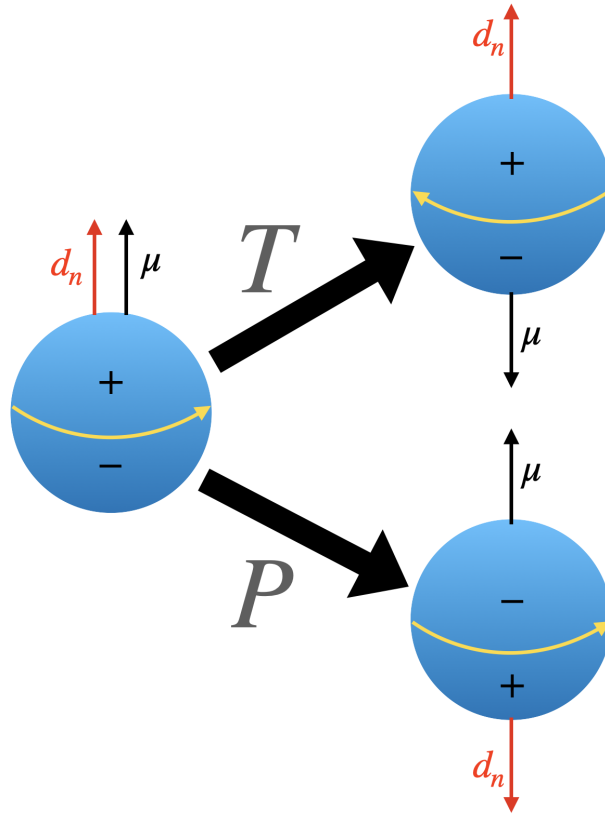


**Figure 1:** The EDM under separate parity (P) and time-reversal (T) transformations.

There are numerous other examples of where BSM physics and LQCD intersect<sup>1</sup>, particularly when one considers non-flavor diagonal processes. In this proceeding only flavor-diagonal CP-violating BSM processes will be considered, and in particular we will look at the quark-chromo EDM operator and the standard  $\theta$ -term of LQCD. For a more general review of these processes the reader is referred to the nice overview given in [6].

This proceeding is organized as follows: in the next section we give a cursory review of the nEDM and its central role in potentially signalling BSM physics. Then in [section 3](#) we discuss the LQCD formalism. In keeping with the spirit of the Ph.D. school and workshop, we concentrate on the symmetries of the system, violation thereof, and their implications. We then discuss the intricacies of renormalization of BSM operators and the extra complications induced by the lattice discretization in [section 4](#). We then show some recent LQCD calculations related to the CP-violating  $\theta$ -term and qCEDM in [section 5](#). We recapitulate in [section 6](#).

## 2. The neutron EDM

CP violation leads to the existence of an electric dipole moment. To see how this occurs, consider [Figure 1](#). Assuming the nucleon has an EDM, which we label as  $d_n$ , we can compare its behavior and that of the nucleon's magnetic moment  $\mu$  under parity (P) and time-reversal (T)

<sup>1</sup> $0\nu\beta\beta$  is another BSM example where LQCD plays a central role. See, e.g. [4, 5] and the proceeding from Davoudi.

transformations. A P-transformation leaves  $\mu$  unchanged, while  $d_n$  switches direction, whereas a T-transformation does the opposite. Thus the system is *not* invariant under either P- or T-transformations, indicating that these symmetries are violated in the presence of a permanent  $d_n$ . Due to overall CPT invariance, this implies that the combined operation of CP is itself violated due to the existence of  $d_n$ .

Conversely, if there are sources of CP-violation, one can expect the existence of a permanent  $d_n$ . Within the Standard Model itself there is CP violation coming from the Cabibbo–Kobayashi–Maskawa (CKM) matrix for weak interactions. However, the amount of CP violation due to the weak interaction is insufficient to explain the observed matter/anti-matter asymmetry. The value of the induced nEDM due to this source of CP violation is predicted to be  $|d_n| \sim 1\text{--}6 \times 10^{-32}$  e-cm [7], which is currently about 6 orders of magnitude below current experimental bound of  $|d_n| < 1.8 \times 10^{-26}$  e-cm [8].

Because of the large separation between the predicted nEDM due to the CKM matrix and current experimental bounds, any definitive measurement of a nEDM larger than the weak prediction in the foreseeable future could originate from either the QCD  $\theta$ -term,

$$-\frac{n_f g^2 \theta}{32\pi^2} F_{\mu\nu} \tilde{F}^{\mu\nu} \quad (1)$$

or BSM sources such as, for example, the qCEDM operator,

$$O_C^{ij}(x) = \bar{\psi}_i(x) \gamma_5 \sigma_{\mu\nu} F_{\mu\nu}(x) \psi_j(x) . \quad (2)$$

The various terms showing up in [Equation 1](#) and [Equation 2](#) will be defined and discussed in more detail in the following section. We only note here that both terms are CP violating, and that the qCEDM operator has scaling (or engineering) dimension of five. Typically BSM operators have dimension five or greater. [Figure 2](#) shows diagrammatic examples of other CP-violating BSM operators.

Any nEDM measurement would provide a clean and precise indication of potential new physics. It is therefore important to predict the pattern of observed EDMs of not only nucleons, but larger nuclei as well as atomic and molecular EDMs, so as to be able to distinguish between different BSM theories and the  $\theta$ -term [9]. Here LQCD is an essential tool in performing the calculations relevant for these predictions.

### 3. Lattice QCD 101

The QCD Lagrangian is based off local SU(3) color symmetry and is given by

$$\mathcal{L}_{\text{QCD}} = -\frac{1}{4} F_{\mu\nu}^a F_a^{\mu\nu} + \bar{\psi}_f (i\not{D} - m_f) \psi_f , \quad (3)$$

where  $\psi_f$  is one of  $N_f$  fermion quark fields with flavor  $f$  that carries both color and spinor degrees of freedom and  $m_f$  is the quark mass of that flavor. Here repeated indices are summed and Roman letters indicate color degrees of freedom and Greek symbols for spinor degrees of freedom. The index  $a$  in this case runs from  $a = 1 \dots 8$ , while the index  $f$  runs from  $f = 1 \dots N_F$ , the number of fermion flavors.

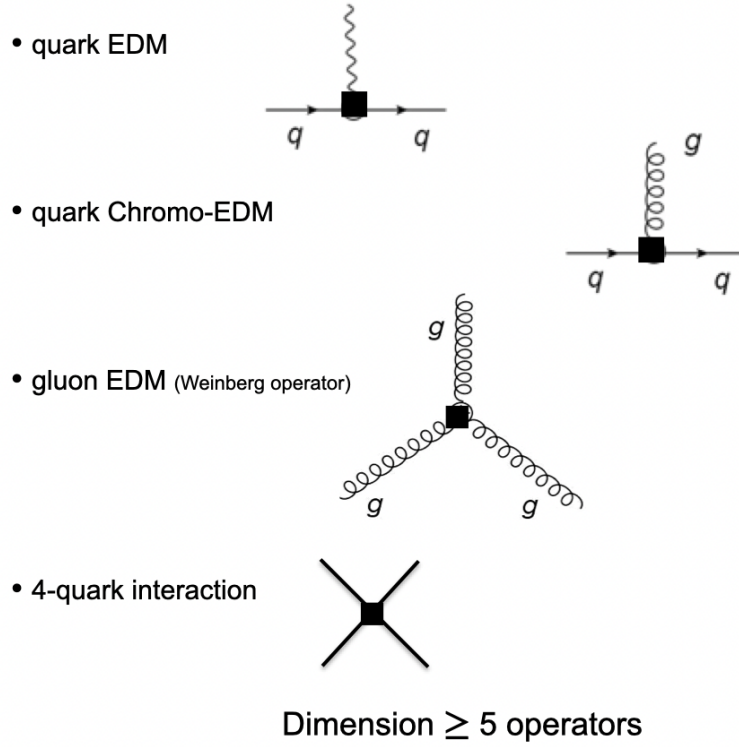


**Figure 2:** Diagrammatic representations of some CP-violating BSM operators.

The field tensor  $F_{\mu\nu}^a$ , describing the kinematics of the gluon gauge fields is

$$F_{\mu\nu}^a = \partial_\mu A_\nu^a - \partial_\nu A_\mu^a - g_0 f_{abc} A_\mu^b A_\nu^c, \quad (4)$$

and the covariant derivative  $\not{D} = \gamma^\mu D_\mu$ , which provides the coupling between the quarks and gluons with coupling strength  $g_0$ , is

$$D_\mu = \partial_\mu \mathbb{1} + ig_0 T^a A_\mu^a, \quad (5)$$

The generators  $T^a$  of SU(3) satisfy the following Lie algebra,

$$[T^a, T^b] = if_{abc} T^c, \quad (6)$$

where  $f_{abc}$  are the structure constants of the group and the generators  $T^a$  consist of 8 matrices of dimension  $3 \times 3$  (see, e.g. [10]). The Lagrangian in Equation 3 is invariant under *local* SU(3) transformations,

$$\psi_f \rightarrow \Lambda_\alpha(x) \psi_f \quad (7)$$

$$A_\mu \rightarrow \Lambda_\alpha(x) A_\mu \Lambda_\alpha^{-1}(x) + \frac{i}{g_0} (\partial_\mu \Lambda_\alpha(x)) \Lambda_\alpha^{-1}(x), \quad (8)$$

where  $\Lambda_\alpha(x)$  is spatially dependent and is an element of SU(3). In the limit when all quark flavors are massless,  $m_f \rightarrow 0$ , the quark content of the Lagrangian in Equation 3 can be written in terms of the left and right helicities of the quark fields  $\psi_{f,L/R}$ ,

$$\bar{\psi}_{f,L} i \not{D} \psi_{f,L} + \bar{\psi}_{f,R} i \not{D} \psi_{f,R} + \mathcal{L}_{\text{gluons}}. \quad (9)$$

In this limit the left and right helicities decouple and the Lagrangian is invariant under separate rotations of any  $N_f \times N_f$  unitary matrix for each helicity. In other words, the Lagrangian processes  $U(N_f)_L \times U(N_f)_R$  chiral (flavor) symmetry.

### 3.1 Discretizing space and time

Lattice QCD calculations are performed in Euclidean, or imaginary, time. The QCD action  $S_M[\bar{\psi}, \psi, A]$  in Minkowski space, defined as the integral over space-time of the Lagrangian in Equation 3, is obtained in Euclidean space by performing the Wick rotation  $t \rightarrow -i\tau$ ,

$$\begin{aligned} S_M &\rightarrow iS_M \equiv S_E \\ &= - \int dx^4 \left( \frac{1}{4} (F_{\mu\nu}^a)^2 + \bar{\psi} (\not{D} + m) \psi \right). \end{aligned} \quad (10)$$

The action in Equation 10 plays a central role in lattice QCD calculations since the expectation value of any operator  $O$  is given by

$$\langle O \rangle = \frac{1}{\mathcal{Z}} \int \mathcal{D}A \mathcal{D}\bar{\psi} \mathcal{D}\psi O[A] \exp \{-S[\bar{\psi}, \psi, A]\} \quad (11)$$

$$= \frac{1}{\mathcal{Z}} \int \mathcal{D}A O[A] \det(M[A]) \exp \left\{ - \int dx^4 \frac{1}{4} (F_{\mu\nu}^a)^2 \right\} \quad (12)$$

$$\equiv \frac{1}{\mathcal{Z}} \int \mathcal{D}A O[A] \det(M[A]) \exp \{-S_G[A]\}, \quad (13)$$

where  $M[A] \equiv \not{D} + m = \sum_{\mu} \gamma_{\mu} D_{\mu} + m$  is the ‘‘fermion matrix’’ obtained by integrating over the fermion fields and

$$\mathcal{Z} = \int \mathcal{D}A \mathcal{D}\bar{\psi} \mathcal{D}\psi \exp \{-S[\bar{\psi}, \psi, A]\}. \quad (14)$$

$\mathcal{Z}$  can be interpreted as a partition function.

In practice the functional integrals in Equation 12 are not analytically possible, and therefore numerical methods are needed. Lattice QCD calculations make use of space-time that is approximated by a discrete hyper-cubic (4-dimensions) lattice, with lattice spacing  $a$  typically of size  $a \sim 0.05 - 0.1$  fm. This corresponds to physical spatial dimensions  $L$  of the cube of order  $L \sim 4 - 6$  fm or larger. Periodic boundary conditions (PBCs) are typically employed at the faces of the spatial cube, while anti-periodic boundary conditions (aPBCs) are used in the temporal directions to account for the anti-symmetry of the fermions. Because of the finite volume, the allowed momentum modes are discrete and given by  $\vec{p}_n = 2\pi\vec{n}/L$ , where  $\vec{n} = (n_x, n_y, n_z)$  are a triplet of integers. The lattice discretization acts as an ultraviolet cutoff to the theory.

### 3.2 The Nielsen-Ninomiya theorem

An implication of the lattice discretization is the presence of extra fermion modes, or ‘fermion doublers’, at the edges of the Brillouin zones. For a naïve discretization one ends up with a total of 16 fermion modes, only one of which is physically relevant. One can add to the lattice action a so called Wilson term<sup>2</sup> that gives these doublers an infinite mass in the continuum limit, thereby decoupling them from the theory in this limit. However such a term breaks chiral symmetry,

<sup>2</sup>See, e.g. [11] for a nice introduction to this topic.

**Table 1:** Cubic volume decomposition in terms of SO(3) irreps.

Cubic irrep $\Gamma$	SO(3) irrep decomposition $l$	$\Gamma$	$l$
$A_1^+$	$l=0,4,6,8,\dots$	$A_1^-$	$l=9,13,15,\dots$
$A_2^+$	$l=6,10,12,\dots$	$A_2^-$	$l=3,7,9,\dots$
$T_1^+$	$l=4,6,8,\dots$	$T_1^-$	$l=1,3,5,7,9,\dots$
$T_2^+$	$l=2,4,6,8,\dots$	$T_2^-$	$l=3,5,7,9,\dots$
$E^+$	$l=2,4,6,8,\dots$	$E^-$	$l=5,7,9,\dots$

and this in turn has implications to the renormalization of the theory. When chiral symmetry *is* preserved, only *multiplicative* renormalizations occur, ie. parameters of the theory pick up an overall multiplicative factor. On the other hand, the breaking of chiral symmetry induces *additive* renormalizations which adds an additional complication.

The connection between chiral symmetry, fermion ‘doublers’, and the lattice discretization is succinctly expressed by the Nielsen-Ninomiya ‘No-Go’ theorem [12], which states that for a discretized theory in even dimensions (e.g. three spatial + one temporal), if the action is local, Hermitian, and chiral and translationally invariant, then it must describe an even number of fermions where there is an equal amount for each chirality. The 16 fermions mentioned above is a consequence of this theorem. Only by violating the assumptions of the theorem, for example by introducing the chiral symmetry-violating Wilson term, can one circumvent this theorem and remove these doublers.

### 3.3 Symmetries of the finite-volume point groups

Since calculations are performed within a finite cubic volume, it is the irreducible representations (irreps) of the cubic, or octahedral, group  $O$  that determine the degeneracies of the eigenstates in the lattice volume. This has direct implications to extracting angular-momentum dependent quantities, such as phase shifts  $\delta_l$  [13]. In the infinite volume limit, angular momenta falls under SO(3) symmetry, which has an infinite number of irreps, each labelled by  $l$  and has dimension  $2l + 1$ . In a cubic volume, the octahedral group has five irreps labelled  $A_1$ ,  $A_2$ ,  $T_1$ ,  $T_2$ , and  $E$ , with dimensions 1, 1, 3, 3, and 2, respectively. The cube is also invariant under parity operations, so each irrep can be further divided as even or odd under parity operations (e.g.  $A_1 \rightarrow A_1^\pm$ ). The spatial component of all lattice-calculated quantities fall under these irreps. The decomposition of cubic groups in terms of SO(3) irreps, some of which are given in table 1, is infinite in dimension. More importantly, the decomposition shows that different angular momenta mix in a cubic volume. If the center of the group is enlarged to  $\mathcal{Z}_2$ , one has the *double cover* of the cubic group,  $O_h$  [14]. Odd-half spin angular momentum can now be represented by three additional irreps,  $G_1^\pm$ ,  $G_2^\pm$ , and  $H$ . As before, the decomposition of these irreps in terms of SU(2) irreps is infinite and mixes SU(2) irreps.

## 4. EFT and renormalization group

There are numerous candidate BSM theories and a description of these theories is beyond the scope of these proceedings. Such theories, however, are dynamically relevant at energy scales

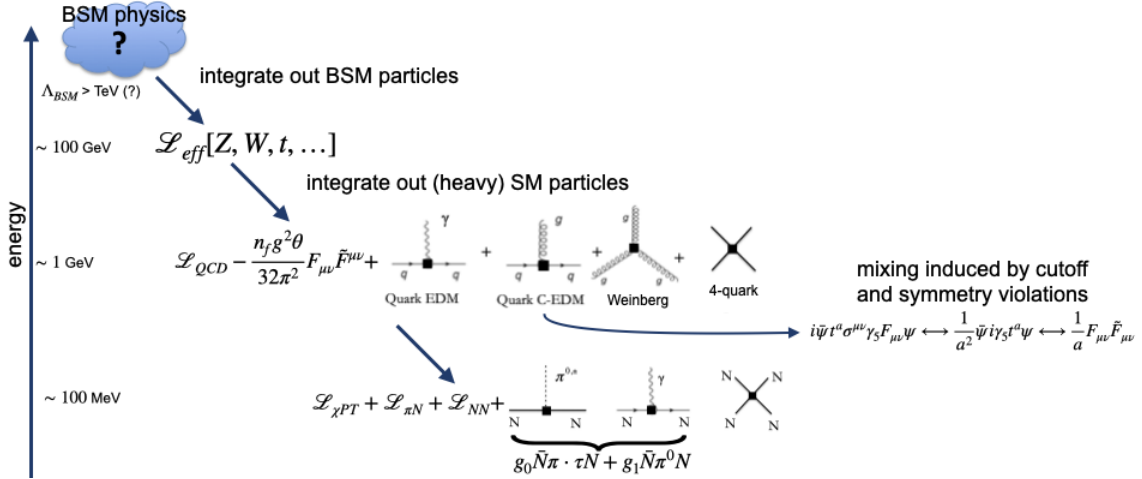


**Figure 3:** Schematic representation of the renormalization group program for obtaining the induced CP-violating BSM operators at the hadronic energy scale.

typically of order  $\Lambda_{BSM} \gtrsim 1$  TeV or more. We, of course, are interested in physics occurring at a much lower scale. We can obtain an effective field theory relevant at lower energy scales by employing the renormalization group. Under renormalization, one ‘integrates out the heavy’ BSM particles to obtain an effective field theory at a lower energy scale. One repeats this integration scheme, integrating out heavy fields that are essentially non-dynamical at the energy scale one is interested in. At the GeV scale, as depicted in Figure 3, one obtains the QCD lagrangian and higher dimension CP-violating effective operators induced by the presence of BSM. Note however, that the form of these effective operators is universal and constrained by symmetries, despite originating from potentially disparate BSM theories. Only their low-energy constants (LECs) dictate their BSM origins. Because of the generality of the CP-violating operators, lattice calculations of these operators can be performed with their unknown LECs as free parameters, to be later fixed by candidate BSM theories. Conversely, a phase-space investigation of these parameters can be done to rule out different BSM theories. A more thorough description of this topic can be found in [15, 16].

#### 4.1 Mixing of operators due to discretization

A lattice-discretised version of these higher-dimension operators, however, can cause mixing of their coefficients with lower-dimension operators [17], leading to unwanted divergences that require sophisticated renormalizations and which make the separation and extraction of BSM observables from standard QCD observables difficult. For example, the quark-CEDM operator, because of the lattice spacing  $a$ , will mix with the pseudo-scale density and the  $\theta$ -term (if present)

$$\underbrace{i\bar{\psi}t^a\sigma^{\mu\nu}\gamma_5 F_{\mu\nu}\psi}_{\text{qCEDM}} \longleftrightarrow \underbrace{\frac{1}{a^2}\bar{\psi}i\gamma_5 t^a\psi}_{\text{pseudo-scalar density}} \longleftrightarrow \underbrace{\frac{1}{a}F_{\mu\nu}\tilde{F}_{\mu\nu}}_{\theta\text{-term}}. \quad (15)$$

Note the inverse power dependence on the lattice spacing  $a$ , which implies that such mixing diverges in the continuum  $a \rightarrow 0$  limit. Such mixing is inevitable, and must be accounted for

and correctly subtracted. We use the gradient flow formalism to address the issues related to these power divergences due to mixing.

## 4.2 Gradient flow

The gradient flow (GF) [18, 19] can be used to circumvent such mixing, as well as to address other issues related to renormalization. The gradient flow [18] of Yang-Mills gauge fields is defined as follows

$$\partial_t B_\mu = D_{\nu,t} G_{\nu\mu}, \quad (16)$$

where the flow time  $t$  has a time-squared dimension,

$$G_{\mu\nu} = \partial_\mu B_\nu - \partial_\nu B_\mu + [B_\mu, B_\nu], \quad D_{\mu,t} = \partial_\mu + [B_\mu, \cdot], \quad (17)$$

and the initial condition on the flow-time-dependent field  $B_\mu(x, t)$  at  $t = 0$  is given by the fundamental gauge field  $F_{\mu\nu}$ .

Field theory can be formally defined in this extra flowed dimension. One finds that power divergences originating from the lattice spacing mixing that occur at flow time  $t = 0$  (the original theory) have much milder behavior at finite flow time, scaling as  $1/t$ . This means that the negative effects of the original power divergences can be mitigated by integrating to larger flow times  $t$ . Finally, by performing the continuum limit at finite flow time, the theory at finite flow time recovers chiral symmetry and therefore only induces multiplicative renormalizations.

## 5. Results for $\theta$ -term and qCEDM

A description of the technical details of an actual lattice calculation involving the operators in Equation 1 and Equation 2 is beyond the scope of these proceedings, and therefore we only comment on their general features. We again refer the reader to the overview given in [6], and references within, for a discussion of the technicalities and calculations done thus far related to these operators.

For the  $\theta$ -term we take advantage of the fact that, though we do not know the actual value of  $\theta$ , we know from experiments that it is very small,  $|\theta| \ll 1$ , and therefore we can perform a Taylor expansion of this term in the action. This means that any expectation value of some operator  $O$  in Equation 12 can then be expanded as

$$\langle O \rangle_\theta = \langle O \rangle + i\theta \langle OQ \rangle + \mathcal{O}(\theta^2), \quad (18)$$

where  $Q$  is the topological term,

$$Q = \frac{a^4}{64\pi^2} \epsilon_{\mu\nu\rho\sigma} \sum_x F_{\mu\nu}^a(x, t_f) F_{\rho\sigma}^a(x, t_f). \quad (19)$$

By analyzing select two- and three-point functions for  $O$  we can extract the nEDM at various values of unphysical pion masses and using chiral EFT we can interpolate to the physical pion point. Figure 4 shows our recent results for the EDM as induced by the  $\theta$ -term, and compares our results to those found in the literature. Combined with the experimental bounds on the nEDM we find that the value of  $\theta$  is constrained to  $|\theta| < 1.98 \times 10^{-10}$  with a 90% confidence level [20].

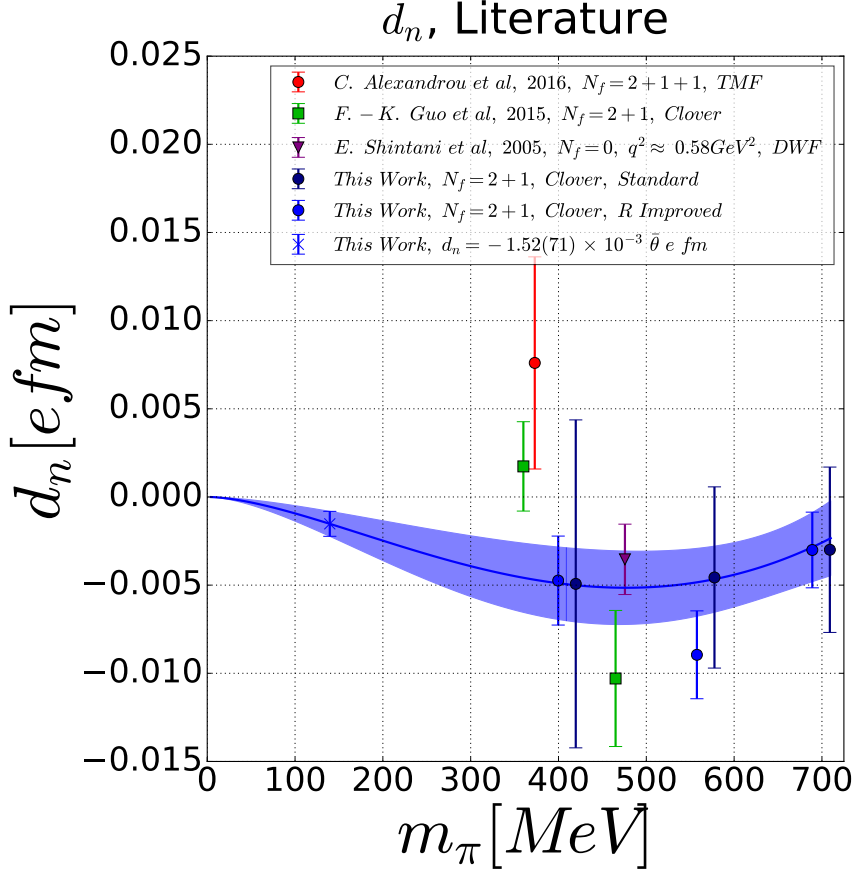


**Figure 4:** Recent results  $d_n$  obtained by the Symlat collaboration [20] compared to other lattice QCD results [21–23]. The light blue bands correspond to a chiral extrapolation.

The calculation of the nEDM as induced by the qCEDM operator is much more complicated because of its mixing with the pseudoscalar density. Indeed, before any prediction for the nEDM can be made, the coupling to the pseudoscalar density must be ascertained so that it can be appropriately subtracted. Fortunately this coupling  $c_{CP}$  can be determined perturbatively in a short flowtime expansion [24],

$$O_C(t) = \frac{c_{CP}(t)}{t} P(0) + \dots, \quad (20)$$

where  $P(0)$  is the pseudo-scalar density at zero flowtime and  $O_C$  is the qCEDM operator. Defining the ratio

$$R_P(t) = t \frac{\langle O_C(t) P(0) \rangle}{\langle P(0) P(0) \rangle}, \quad (21)$$

and using the short flow-time expansion of the qCEDM given in Equation 20, we have

$$R_P(t) = c_{CP} + a \frac{t_0}{t} + b \frac{t}{t_0}, \quad (22)$$

where  $t_0$  is some fiducial flowtime scale. We have performed various calculations of  $R_P(t)$  at different values of the flow time  $t$  to determine the parameters  $a$ ,  $b$ , and the  $c_{CP}$ , and matched

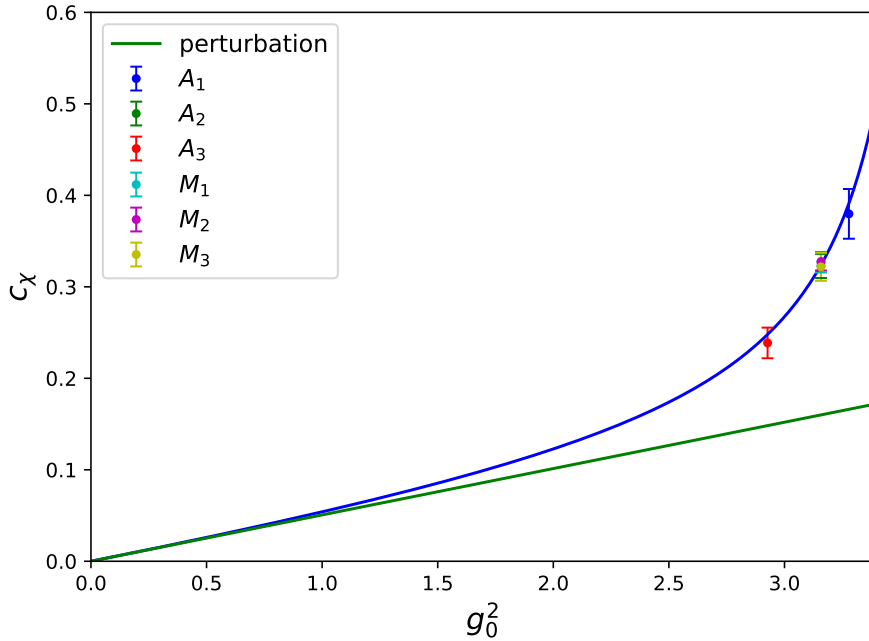


**Figure 5:** Non-perturbative dependence of the expansion coefficient  $c_\chi = \frac{t}{Z_\chi} c_{CP}$  as a function of the bare coupling  $g_0^2$ , obtained from calculations using different lattice ensembles  $A_i$  and  $M_i$  defined in [25]. The curve represents a Padé approximant of the data with the constraint imposed by a perturbative calculation (straight line) done in [24].

our results onto perturbation theory to determine the dependence of  $c_{CP}$  on the coupling  $g_0$  of the theory [25]. Our results are shown in Figure 5, where we express our results as a function of the coupling  $g_0$  and the coupling as  $c_\chi = \frac{t}{Z_\chi} c_{CP}$ . With this determination of the coupling in hand, the mixing with the pseudoscalar density can now be appropriately subtracted and the nEDM induced by the qCEDM operator deduced. Such calculations of the nEDM are forthcoming.

## 6. Conclusion

Any direct measurement of a nuclear EDM in the near future could arise from the  $\theta$ -term of QCD or signal the presence of BSM physics that violates CP. Such signals would inevitably be small and thus masked by large hadronic processes. Therefore a careful accounting of the hadronic component must be made and this can only be done through lattice QCD.

In this proceeding we gave a short introduction to LQCD and its symmetries. We discussed how symmetry constrains various physical quantities and how CP-violation leads to the existence of a permanent EDM. We then showed how LQCD is used to determine the nEDM induced by various flavor-diagonal CP-violating terms. We concentrated on the  $\theta$ -term of QCD and the quark-chromo EDM operator. In the latter case we demonstrated how the gradient flow was used to tame the power divergences in the inverse lattice spacing due to operator mixing. We showed some recent results from LQCD of the induced nEDM due to the  $\theta$ -term of QCD and the determination of the pseudoscalar coupling with the qCEDM operator.

## Acknowledgement

We thank the members of SymLat, and in particular, Andrea Shindler and Jangho Kim, for their work in this subject area. Indeed, the results presented here were made possible by their hard work. This work was funded in part by the NSFC and the Deutsche Forschungsgemeinschaft (DFG, German Research Foundation) through the funds provided to the Sino-German Collaborative Research Center “Symmetries and the Emergence of Structure in QCD” (NSFC Grant No. 12070131001, DFG Project-ID 196253076 – TRR110). The author gratefully acknowledge the computing time granted by the JARA Vergabegremium and provided on the JARA Partition part of the super-computer JURECA at Forschungszentrum Jülich.

## References

- [1] A. Keshavarzi, K.S. Khaw and T. Yoshioka, *Muon  $g-2$ : A review*, *Nucl. Phys. B* **975** (2022) 115675 [2106.06723].
- [2] MUON  $g-2$  collaboration, *Final Report of the Muon E821 Anomalous Magnetic Moment Measurement at BNL*, *Phys. Rev. D* **73** (2006) 072003 [hep-ex/0602035].
- [3] MUON  $g-2$  collaboration, *Measurement of the Positive Muon Anomalous Magnetic Moment to 0.46 ppm*, *Phys. Rev. Lett.* **126** (2021) 141801 [2104.03281].
- [4] A. Nicholson et al., *Heavy physics contributions to neutrinoless double beta decay from QCD*, *Phys. Rev. Lett.* **121** (2018) 172501 [1805.02634].
- [5] Z. Davoudi and S.V. Kadam, *Path from Lattice QCD to the Short-Distance Contribution to  $0\nu\beta\beta$  Decay with a Light Majorana Neutrino*, *Phys. Rev. Lett.* **126** (2021) 152003 [2012.02083].
- [6] A. Shindler, *Flavor-diagonal CP violation: the electric dipole moment*, *Eur. Phys. J. A* **57** (2021) 128.
- [7] C.-Y. Seng, *Reexamination of The Standard Model Nucleon Electric Dipole Moment*, *Phys. Rev. C* **91** (2015) 025502 [1411.1476].
- [8] C. Abel et al., *Measurement of the Permanent Electric Dipole Moment of the Neutron*, *Phys. Rev. Lett.* **124** (2020) 081803 [2001.11966].
- [9] W. Dekens, J. de Vries, J. Bsaisou, W. Bernreuther, C. Hanhart, U.-G. Meißner et al., *Unraveling models of CP violation through electric dipole moments of light nuclei*, *JHEP* **07** (2014) 069 [1404.6082].
- [10] H. Georgi, *LIE ALGEBRAS IN PARTICLE PHYSICS. FROM ISOSPIN TO UNIFIED THEORIES*, vol. 54 (1982).
- [11] C. Gattringer and C.B. Lang, *Quantum chromodynamics on the lattice*, vol. 788, Springer, Berlin (2010), 10.1007/978-3-642-01850-3.

- [12] H.B. Nielsen and M. Ninomiya, *No Go Theorem for Regularizing Chiral Fermions*, *Phys. Lett. B* **105** (1981) 219.
- [13] T. Luu and M.J. Savage, *Extracting Scattering Phase-Shifts in Higher Partial-Waves from Lattice QCD Calculations*, *Phys. Rev. D* **83** (2011) 114508 [1101.3347].
- [14] M. Tinkham, *Group Theory and Quantum Mechanics*, Dover Books on Chemistry and Earth Sciences, Dover Publications (2003).
- [15] E. Mereghetti, J. de Vries, W.H. Hockings, C.M. Maekawa and U. van Kolck, *The Electric Dipole Form Factor of the Nucleon in Chiral Perturbation Theory to Sub-leading Order*, *Phys. Lett.* **B696** (2011) 97 [1010.4078].
- [16] J. Bsaisou, J. de Vries, C. Hanhart, S. Liebig, U.-G. Meissner, D. Minossi et al., *Nuclear Electric Dipole Moments in Chiral Effective Field Theory*, *JHEP* **03** (2015) 104 [1411.5804].
- [17] T. Bhattacharya, V. Cirigliano, R. Gupta, E. Mereghetti and B. Yoon, *Dimension-5 CP-odd operators: QCD mixing and renormalization*, *Phys. Rev. D* **92** (2015) 114026 [1502.07325].
- [18] M. Lüscher, *Properties and uses of the Wilson flow in lattice QCD*, *JHEP* **1008** (2010) 071 [1006.4518].
- [19] M. Lüscher, *Chiral symmetry and the Yang–Mills gradient flow*, *JHEP* **1304** (2013) 123 [1302.5246].
- [20] J. Dragos, T. Luu, A. Shindler, J. de Vries and A. Yousif, *Confirming the Existence of the strong CP Problem in Lattice QCD with the Gradient Flow*, *Phys. Rev. C* **103** (2021) 015202 [1902.03254].
- [21] C. Alexandrou, A. Athenodorou, M. Constantinou, K. Hadjiyiannakou, K. Jansen, G. Koutsou et al., *Neutron electric dipole moment using  $N_f = 2 + 1 + 1$  twisted mass fermions*, *Phys. Rev.* **D93** (2016) 074503 [1510.05823].
- [22] F.K. Guo, R. Horsley, U.G. Meissner, Y. Nakamura, H. Perlt, P.E.L. Rakow et al., *The electric dipole moment of the neutron from 2+1 flavor lattice QCD*, *Phys. Rev. Lett.* **115** (2015) 062001 [1502.02295].
- [23] E. Shintani, S. Aoki, N. Ishizuka, K. Kanaya, Y. Kikukawa, Y. Kuramashi et al., *Neutron electric dipole moment from lattice QCD*, *Phys. Rev.* **D72** (2005) 014504 [hep-lat/0505022].
- [24] SYMLAT collaboration, *Short flow-time coefficients of CP-violating operators*, *Phys. Rev. D* **102** (2020) 034509 [2005.04199].
- [25] SYMLAT collaboration, *Nonperturbative renormalization of the quark chromoelectric dipole moment with the gradient flow: Power divergences*, *Phys. Rev. D* **104** (2021) 074516 [2106.07633].